American Mineralogist, Volume 84, pages 1613–1621, 1999

Tobermorites: Their real structure and order-disorder (OD) character

STEFANO MERLINO,[1,*] ELENA BONACCORSI,[1] AND THOMAS ARMBRUSTER[2]

[1]Dipartimento di Scienze della Terra, Università di Pisa, Italy
[2]Laboratorium für chemische und mineralogische Kristallographie, Universität Bern, Switzerland

ABSTRACT

The real structures of clinotobermorite, tobermorite 9 Å, and tobermorite 11 Å were determined through the application of OD approach, which allowed us to explain their peculiar disorder and polytypic features and to derive the main polytypes for each of them. The structural arrangements will be described and discussed for one polytype of each compound: clinotobermorite, triclinic polytype $C1$, $a = 11.274$, $b = 7.344$, $c = 11.468$ Å, $\alpha = 99.18°$, $\beta = 97.19°$, $\gamma = 90.03°$; tobermorite 9 Å, triclinic polytype $C\bar{1}$, $a = 11.156$, $b = 7.303$, $c = 9.566$ Å, $\alpha = 101.08°$, $\beta = 92.83°$, $\gamma = 89.98°$; tobermorite 11 Å, monoclinic polytype $B11m$, $a = 6.735$, $b = 7.385$, $c = 22.487$ Å, $\gamma = 123.25°$. Common structural features are infinite layers, parallel to (001), formed by sevenfold-coordinated calcium polyhedra. Tetrahedral double chains, built up through condensation of "Dreiereinfachketten" of wollastonite-type and running along **b**, link together adjacent calcium layers in clinotobermorite and tobermorite 11 Å, whereas single tetrahedral chains connect adjacent calcium layers in tobermorite 9 Å. The relatively wide channels of clinotobermorite and tobermorite 11 Å host "zeolitic" calcium cations and water molecules. The present structural results now allow for a sound discussion of the crystal chemical relationships between the various members of the tobermorite group and an explanation of the peculiar thermal behavior of tobermorite 11 Å.

INTRODUCTION

Among the numerous hydrated calcium silicates occurring in nature as hydrothermal alteration products of calcium carbonate rocks and as vesicle fillings in basalts, particular attention has been given to the family of tobermorite. Four members have been so far sufficiently characterized for chemical composition, crystallographic properties, and reciprocal relationships: clinotobermorite, tobermorite 9 Å, tobermorite 11 Å, and tobermorite 14 Å. The notations 9 Å, 11 Å, and 14 Å refer to the characteristic basal spacings of 9.3, 11.3, and 14.0 Å, which these phases present in their X-ray powder diffraction patterns. By heating tobermorite 14 Å, tobermorite 11 Å and subsequently tobermorite 9 Å are obtained through progressive dehydration processes. However, some specimens of tobermorite 11 Å do not shrink on heating and are called "anomalous," whereas those specimens that shrink on heating are called "normal."

The particular interest in the structure and crystal chemistry of the minerals of tobermorite group stemmed from their close relationships with the CSH (hydrated calcium silicates) phases formed during the hydration processes of Portland cement (Taylor 1964, 1992, 1997). Subsequently attention has been drawn to the properties of tobermorite as a cation exchanger and its potential applications in catalysis and in nuclear and hazardous waste disposal (Komarneni and Roy 1983). Therefore, a broad series of studies have been carried on with different techniques and approaches with the aim to acquire a deep knowledge of the structural aspects and crystal chemical features of tobermorite minerals, with special consideration of tobermorite 11 Å for its central role in the family and the ambiguity of its behavior in the dehydration processes.

Although some basic structural features were already known since the first study by Megaw and Kelsey (1956), a clear and definite understanding of the complete structural assessment had not been obtained. The main difficulty, besides the small dimensions of the crystals which are generally unsuitable for single crystal X-ray diffraction experiments, is related to the extensive disorder displayed by all the minerals in this group. Here we describe the peculiar kind of disorder taking place in these natural phases and indicate how it was possible to unravel their "real" structures, to define the structural relationships between the various phases and to present a reliable explanation of the enigmatic behavior of tobermorite 11 Å in the dehydration process.

ORDER-DISORDER STRUCTURES

The diffraction patterns of all the phases in the tobermorite group display features characteristic of OD structures consisting of equivalent layers. In OD structures, neighboring layers can be arranged in two or more geometrically equivalent ways. The existence of two or more different ways of connecting neighboring layers makes it possible to obtain a family of structures with variable degree of order, which, taken as a whole, build up a family of OD structures. The symmetry features common to all the members are dealt with by the OD theory

* E-mail: merlino@dst.unipi.it

(Dornberger-Schiff 1956, 1964, 1966; Ďurovič 1997; Merlino 1997), which focuses attention on the space transformations which convert any layer into itself or into the adjacent one. Such space transformations are the so-called λ- and σ-POs (partial operations), respectively, which, as suggested by their name, are not necessarily valid for the whole structure.

The common symmetry properties of a whole family are fully described by a symbol as:

$$\begin{matrix} P\ m \quad m\ (2) \\ \{n_{s,2}\ n_{2,r}\ (2_2)\} \end{matrix} \qquad (1)$$

The first line presents the λ-operations (symmetry operations of the single layer, corresponding to one of the 80 layer groups), the second line presents the σ-operations. The parentheses in the third position of each line indicate that only the basic vectors **a** and **b** are translation vectors corresponding to the periodicities of the single layer, whereas the third vector $\mathbf{c}_0$ is not a translation vector. In the example the single layer has primitive lattice, mirror planes normal to **a** and to **b** and a twofold axis parallel to $\mathbf{c}_0$. The σ-operations (second line) are: *n* glide normal to **a**, with translational component $s\mathbf{b}/2 + \mathbf{c}_0$; *n* glide normal to **b**, with translational component $\mathbf{c}_0 + r\mathbf{a}/2$; a screw with translational component $\mathbf{c}_0$. It seems proper to recall that the most general glide operation is denoted $n_{r,s}$: the order of the indices in the symbol is chosen in such way that the directions to which *n* and the two indices refer follow each other in a cyclic way. The indices *r* and *s* are only of interest *modulo* 2, namely *r* may be replaced by $r + 2$ or $r - 2$ and similarly *s* by $s + 2$ and $s - 2$ without change or meaning.

The various disordered and ordered structures display diffraction patterns with common features (family reflections: reflections which present the same position and intensities in all the OD structures of the family) and can be distinguished for the position and intensities of the other reflections. The family reflections are always sharp, whereas the other reflections may be more or less diffuse, sometimes appearing as continuous streaks. The family reflections correspond to a fictitious structure, periodic in three dimensions, closely related to the structures of the family and called "family structure." Two basic vectors of the family structure are chosen collinear with the translation vectors of the single layer. If, as in the example here presented, the translation vectors are **a** and **b**, the vectors **A**, **B**, **C** of the family structure are such that: $\mathbf{a} = q\mathbf{A}$, $\mathbf{b} = t\mathbf{B}$, and $\mathrm{C} = p\mathbf{c}_0$, with *q*, *t*, and *p* integer numbers.

The knowledge of the family structure, which is more loosely called "average structure" or "sub-cell structure," is an important but not sufficient step towards the full understanding of the structural features of the family. The systematic application of the OD procedures may be extremely helpful in passing from the average to the real structure. To this effect, OD theory (1) indicates which sets of operations connecting adjacent layers (σ-operations) are compatible with the symmetry operations of the single layer (λ-operations); (2) indicates how to select the correct λ- and σ-operations among the various possibilities: in fact both λ- and σ-operations are reflected in the symmetry operations of the "family structure"; and (3) permits to enumerate and derive the MDO structures (structures with maximum degree of order: in them not only pairs but also triples, quadruples,.....*n*-ples of layers are geometrically equivalent), corresponding to the main and most frequently occurring polytypes in the family, and presents their cell parameters and symmetry properties.

THE OD CHARACTER OF CLINOTOBERMORITE AND DERIVATION OF THE MDO POLYTYPES

Clinotobermorite was first found as a new natural phase at Fuka, Okayama Prefecture, Japan, by Henmi and Kusachi (1992) who studied its chemical and crystallographic properties; crystals from a second occurrence (Wessels mine, Kalahari manganese field, South Africa) were studied by Hoffmann and Armbruster (1997). The OD character of clinotobermorite is clearly displayed by the diffraction pattern (streaks, diffuse reflections, unusual absence rules) described for both specimens.

The pattern may be referred to a unit cell with parameters: $a = 11.27$, $b = 7.34$, $c = 22.64$ Å, $\beta = 97.28°$, thus showing the 7.3 Å translation, which is typical of several CSH minerals. Moreover, both groups of authors indicated a *C* centering, with reference to this unit cell, and maintained that whereas the reflections with $k = 2n$ were always sharp, continuous streaks parallel to **c***, or diffuse maxima on rows parallel to **c***, were found for $k = 2n + 1$.

Appreciation of the symmetry properties of the OD family requires the knowledge of the symmetry of the building structural layers, as well as the symmetry operations which relate adjacent layers, a knowledge which may often be obtained through a careful scrutiny of the diffraction patterns with attention to the systematic absences in the family reflections and in the whole diffraction pattern. For the present case, we observed: (1) the *C* centering condition, valid for all the reflections, namely $h + k = 2n$; and (2) a condition valid for reflections with $k = 2n$ (and therefore $h = 2n$), which are present only for $k + 2l = 4n$.

Condition 2 becomes an ordinary rule for reflections with $k = 2K$ (and thus $h = 2H$) considered for themselves. These reflections correspond to a reciprocal lattice with vectors **A*** **B*** **C*** related to the vectors **a*** **b*** **c*** in this way: $\mathbf{A}^* = 2\mathbf{a}^*$, $\mathbf{B}^* = 2\mathbf{b}^*$, $\mathbf{C}^* = \mathbf{c}^*$. For these reflections (which are the family reflections) the Condition 2 becomes: reflections *HKL* are present for $K + L = 2n$, which corresponds to *A* centering of the lattice of the "family" structure.

The "average" or "family" structure, with space group symmetry *A*2/*m*, and $A = 5.638$, $B = 3.672$, $C = 22.636$ Å, $\beta = 97.28°$, was determined by Hoffmann and Armbruster (1997). Their results present the actual arrangement of the calcium "octahedral" sheets, which have the same subperiod, 3.67 Å, of the "family" structure, and indicate the presence of tetrahedral chains of wollastonite type. These results point to a building layer with *C*2/*m* symmetry [more precisely *C*12/*m*(1)] and basis vectors **a**, **b** (translation vectors of the layer, with $a = 11.27$, $b = 7.34$ Å), and $\mathbf{c}_0$ ($c_0 = c/2 = 11.32$ Å; $\beta = 97.28°$), as shown in Figure 1. In Figure 1, the $[Si_3O_9]$ chains are condensed to give double chains; however the same layer symmetry would be obtained if single chains occur, with facing chains displaced by $b/2$.

For layer symmetry *C*12/*m*(1) there are two possible OD groupoid families:

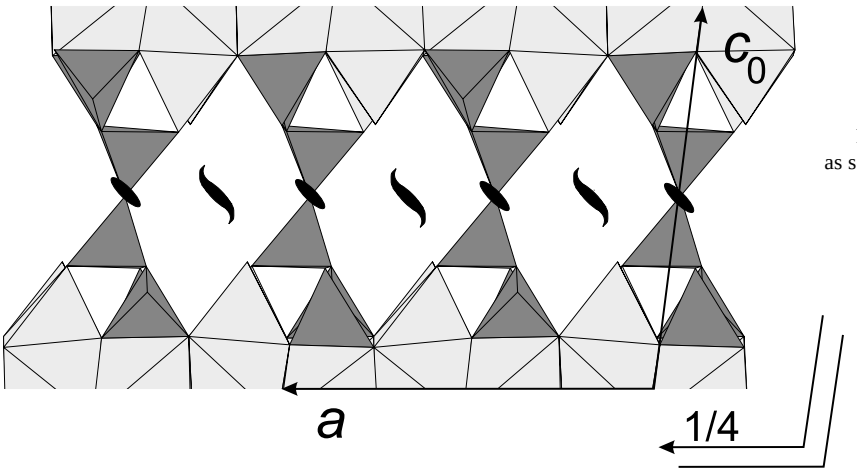

FIGURE 1. Single layer in clinotobermorite, as seen along **b** (**a** horizontal).

$$C \quad 1 \quad 2/m \quad (1) \qquad (2)$$
$$\{\ 1 \quad 2_s/c_2 \quad (1)\ \},$$

or

$$C \quad 1 \quad 2/m \quad (1)$$
$$\{\ 2_r/n_{s,2} \quad 1 \quad (2_2/n_{r,s})\ \} \qquad (3)$$

In facrt, the λ and σ operations of the single layer should correspond to the operators of the family structure, once the translational components of any glide and screw are modified in agreement with the passing from the dimensions of the single layer to the dimensions of the subcell. In our case the single layer has basis vectors **a** and **b** (translation vectors) and $\mathbf{c}_0$, whereas the family structure has translations **A** = **a**/2, **B** = **b**/2, **C** = 2 $\mathbf{c}_0$[1]($q = t = 2$; $p = 2$). Therefore, we have to double the translational components which refer to the **b** axis and to divide by two the translational components which refer to the **c** axis in the OD groupoid family (2), to obtain, with $s = 1/2$, the operators 2, *m*, 2_1, and *c* of the space group *A*2/*m* of the family structure. According to the OD groupoid family so derived,

$$C \quad 1 \quad 2/m \quad (1)$$
$$\{\ 1 \quad 2_{1/2}/c_2 \quad (1)\ \} \qquad (4)$$

[1]This relation, which gives the number *p* of layers for each C translation (in general, for the translation in the direction of missing periodicity) in the "family structure," may be derived without any previous knowledge of the structure. According to Dornberger-Schiff and Fichtner (1972), *p* is the product of three factors: $p = p_1.p_2.p_3$, where p_1 depends on the category of the OD structure (1 for categories I and II, 2 for category III); p_2 depends on the isogonality relationships of operations in two lines of the family symbol (in the present case, first and second lines of the first OD groupoid family in (2) are isogonal and $p_2 = 1$); p_3 depends on the Bravais lattice of the "family structure" (with the orientation assumed in the present case, $p_3 = 1$ for *P* and *C* centered lattices, whereas $p_3 = 2$ for *A*, *B*, *I*, and *F* centered lattices). Therefore in the case under study (category I, isogonality, *A* centering) $p = 2$.

layers with *C*2/*m* symmetry may follow each other in the **c** direction, related by the operator $2_{-1/2}$ or by the operator $2_{1/2}$. Pairs of layers related in one or in the other way are geometrically equivalent: infinite ordered or disordered sequences of layers may occur, corresponding to the infinite possible sequences of the operators $2_{-1/2}$ and $2_{1/2}$. For all the possible sequences, as usual in OD structures, the family reflections, namely those with $k = 2n$, are sharp with constant values (Merlino 1997). The reflections with $k = 2n + 1$ vary (in position, shape, and intensity) depending on the sequence, giving rise to continuous streaks along **c*** for fully disordered sequences. Among the infinite possible ordered sequences (polytypes), OD approach singles out those in which not only pairs, but triples, quadruples,...*n*-ples of layers are geometrically equivalent (MDO polytypes). Two MDO polytypes are possible in this family: (1) MDO_1, corresponding to the sequence in which the operators regularly alternate: $2_{-1/2}$ / $2_{1/2}$ / $2_{-1/2}$ / $2_{1/2}$ / ... and (2) MDO_2, corresponding to the sequence in which one operator is constantly active: $2_{-1/2}$ / $2_{-1/2}$ / $2_{-1/2}$/.... (the sequence $2_{1/2}$ / $2_{1/2}$ / $2_{1/2}$ /.... corresponds to the twin structure).

Symmetry of the MDO_1 polytype in clinotobermorite

Figure 2a shows that (1) the partial glide c_2 between L_2 and L_3 layer is continuing that act between L_1 and L_2 layer; therefore it becomes a total operator *c*, in a structure with a parameter $c = 2c_0$; (2) due to the relative position of the successive layers, the operator 2 (|| **b**) (λ operator of the single layers) is a total operator, valid for the whole structure; and (3) the translation operator **a**/2 + **b**/2 is valid for all the layers. Therefore the whole structure has symmetry *C*2/*c*, with cell parameters: $a = 11.27$, $b = 7.34$, $c = 22.64$ Å, $\beta = 97.2°$.

Symmetry of MDO_2 polytype in clinotobermorite

Figure 2b shows that (1) the partial glide c_2 between L_2 and L_3 layer does not continue that act between L_1 and L_2 layers; it is not a total operator; (2) due to the relative position of the successive layers, the operator 2 (|| b) is not valid for the whole structure; (3) both λ and σ inversion centers are total opera-

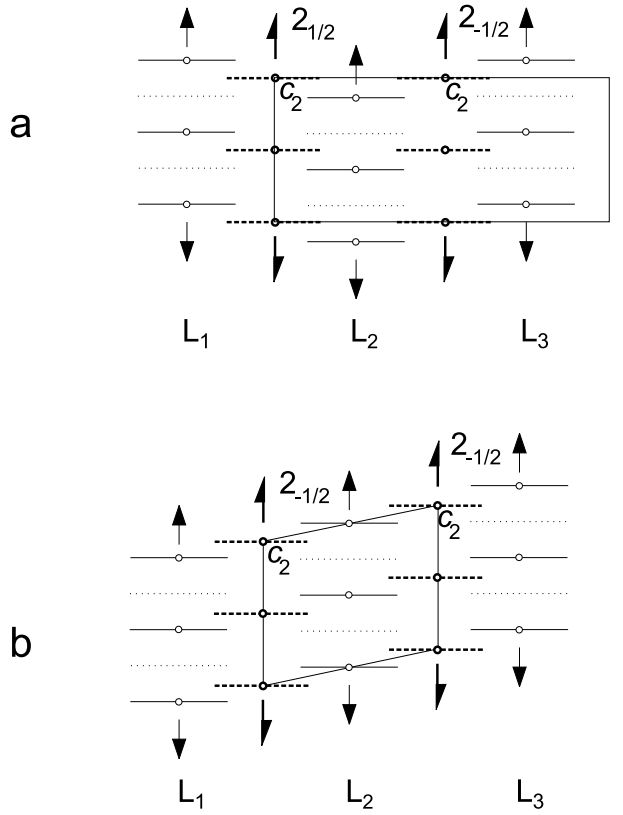

FIGURE 2. Sequences of λ-operators (light marks) and σ–operators (heavy marks) in the monoclinic MDO_1 (**a**) and triclinic MDO_2 (**b**) structures of clinotobermorite, as seen along **a** (**b vertical**); modified from Merlino (1997).

tors; and (4) the translation operator **a**/2 + **b**/2 is valid for all the layers. Therefore the whole structure has $C\bar{1}$ symmetry, with cell parameters: a = 11.27, b = 7.34, c = 11.47 Å, α = 99.2°, β = 97.2°, γ = 90.0°.

The relation between the two MDO structures, and more generally among the various polytypes in the family, may be easily appreciated by observing that layers related by the operators $2_{-1/2}$ and $2_{1/2}$ are translationally equivalent and related by stacking vectors:

$$\mathbf{t}_1 = \mathbf{c}/2 - \mathbf{b}/4 \text{ and } \mathbf{t}_2 = \mathbf{c}/2 + \mathbf{b}/4 \qquad (5)$$

respectively. In the monoclinic polytype the two stacking vectors regularly alternate, whereas in the triclinic polytype the vector $\mathbf{t}_1$ is constantly applied (the constant application of vector $\mathbf{t}_2$ gives rise to the twin structure). The general discussion of the diffractional effects in the whole family (Merlino 1997) is made easier by the translational equivalence of the layers.

STRUCTURAL FEATURES OF CLINOTOBERMORITE

The crystals of clinotobermorite from the Wessels mine were characterized by the presence of domains of both polytypes. We carried out collection of X-ray diffraction data for both polytypes, using a Siemens P4 diffractometer (50 kV, 40 mA) and graphite monochromatized Mo$K\alpha$ radiation (λ = 0.71073 Å). The models were refined to R values of 0.120 [2673 reflections with $F_o > 4\sigma(F_o)$] and R = 0.150 [1930 reflections with $F_o > 4\sigma(F_o)$] for the triclinic and monoclinic polytypes, respectively. The final refinements have been carried out in the space groups $C1$ and Cc, respectively: the lower symmetry, with respect to the OD models, is connected to ordering of Ca cations and water molecules in the channels of the structure. The results obtained with the triclinic form, with a = 11.274(2), b = 7.344(1), c = 11.468(2) Å, α = 99.18(1)°, β = 97.19(1)°, γ = 90.03(1)°, are in Tables 1 (atomic coordinates) and 2 (bond distances) and in Figure 3; the results obtained with the monoclinic form are quite similar. The structure may be described as built up by the following components: (1) infinite layers, parallel to (001), formed by sevenfold-coordinated calcium polyhedra, which are arranged in columns running along **b**. These layers have been excellently described by Hoffmann and Armbruster (1997) in their study of the "subcell structure": each Ca polyhedron has a pyramidal part on one side and a dome part on the other side; the apical sites of the pyramids are placed on opposite sides of the layer in adjacent columns and, in each column, water molecules (W6 and W6A) and oxygen anions (O6 and O6A) regularly alternate on these sites. The chemical nature of O6 and O6A is clearly indicated by their valence bond sums, taking into account, in the case of O6A, that it is acceptor of two strong hydrogen bonds with W7 and W8. (2) Tetra-

TABLE 1. Atomic coordinates and isotropic thermal parameters of clinotobermorite, triclinic polytype, space group $C1$

Atom	x	y	z	U_{iso}
Si1	0.8931(5)	0.2046(7)	0.1839(4)	0.0014(5)
Si1A	–0.8941(5)	–0.2096(7)	–0.1841(4)	0.0014(5)
Si2	0.9963(6)	–0.0362(8)	0.3553(5)	0.0056(5)
Si2A	–0.9950(6)	0.0383(8)	–0.3608(5)	0.0056(5)
Si3	0.8949(5)	–0.3726(7)	0.1869(4)	0.0018(5)
Si3A	–0.8946(5)	0.3688(7)	–0.1859(4)	0.0018(5)
O1	0.913(2)	0.124(2)	0.310(1)	0.013(1)
O1A	–0.916(2)	–0.128(2)	–0.309(1)	0.013(1)
O11	0.919(1)	–0.229(2)	0.316(1)	0.010(1)
O11A	–0.912(1)	0.227(2)	–0.309(1)	0.010(1)
O2	0.771(1)	–0.343(2)	0.115(1)	0.004(1)
O2A	–0.767(1)	0.348(2)	–0.108(1)	0.004(1)
O21	0.765(2)	0.149(2)	0.106(1)	0.008(1)
O21A	–0.767(2)	–0.151(2)	–0.111(1)	0.008(1)
O3	0.005(1)	–0.355(2)	0.111(1)	0.005(1)
O3A	0.003(1)	0.357(2)	–0.106(1)	0.005(1)
O31	0.002(1)	0.155(2)	0.099(1)	0.004(1)
O31A	0.005(1)	–0.161(2)	–0.105(1)	0.004(1)
O4	0.891(1)	0.431(2)	0.237(1)	0.009(1)
O4A	–0.895(1)	–0.432(2)	–0.238(1)	0.009(1)
O5	0.009(2)	–0.002(2)	0.497(1)	0.014(2)
O6	0.127(2)	–0.041(2)	0.311(1)	0.014(2)
O6A	–0.124(2)	0.053(2)	–0.319(1)	0.014(2)
W6	–0.335(4)	–0.051(6)	–0.683(4)	0.092(7)
W6A	0.342(4)	0.043(5)	0.699(4)	0.092(7)
Ca1	0.3640(3)	0.1072(4)	0.9228(3)	0.0023(4)
Ca1A	–0.3634(3)	–0.1042(4)	–0.9134(3)	0.0023(4)
Ca3	0.8679(3)	0.0998(4)	0.8981(3)	0.0024(4)
Ca3A	–0.8711(3)	–0.1001(5)	–0.9069(3)	0.0024(4)
Ca2	0.3113(5)	–0.0177(7)	0.4289(5)	0.025(1)
W5	0.514(2)	0.009(3)	0.511(2)	0.023(3)
W7	0.260(3)	–0.238(4)	0.537(2)	0.054(6)
W8	0.260(3)	0.257(4)	0.535(2)	0.057(7)

TABLE 2. Selected bond distances (in angstroms) in triclinic clinotobermorite

Si1–O1	1.64(2)	Si2–O1	1.61(2)	Si3–O11	1.67(2)
Si1–O21	1.61(2)	Si2–O11	1.63(2)	Si3–O2	1.57(2)
Si1–O31	1.66(1)	Si2–O5	1.59(2)	Si3–O3	1.61(2)
Si1–O4	1.68(2)	Si2–O6	1.62(2)	Si3–O4	1.63(2)
Si1A–O1A	1.63(2)	Si2A–O1A	1.66(2)	Si3A–O11A	1.61(2)
Si1A–O21A	1.60(2)	Si2A–O11A	1.66(2)	Si3A–O2A	1.62(2)
Si1A–O31A	1.55(2)	Si2A–O5	1.62(2)	Si3A–O3A	1.57(2)
Si1A–O4A	1.65(2)	Si2A–O6A	1.59(2)	Si3A–O4A	1.67(2)
Ca1–O2	2.53(1)	Ca3–O2A	2.38(2)	Ca2–O4	2.46(2)
Ca1–O2A	2.35(1)	Ca3–O21	2.75(2)	Ca2–O6	2.32(2)
Ca1–O21A	2.35(2)	Ca3–O21A	2.38(2)	Ca2–W5	2.36(2)
Ca1–O3	2.49(1)	Ca3–O3A	2.43(1)	Ca2–W7	2.31(3)
Ca1–O3A	2.42(1)	Ca3–O31	2.57(1)	Ca2–W8	2.30(3)
Ca1–O31A	2.41(1)	Ca3–O31A	2.46(1)		
Ca1–W6A	2.52(4)	Ca3–O6A	2.47(2)	Ca2–O1	3.06(2)
				Ca2–O11	2.98(2)
Ca1A–O2	2.35(1)	Ca3A–O2	2.44(1)	Ca2–W6A	3.03(4)
Ca1A–O2A	2.57(1)	Ca3A–O21	2.41(2)		
Ca1A–O21	2.33(2)	Ca3A–O21A	2.72(2)		
Ca1A–O3	2.36(1)	Ca3A–O3	2.39(1)		
Ca1A–O3A	2.49(1)	Ca3A–O31	2.35(1)		
Ca1A–O31	2.36(1)	Ca3A–O31A	2.49(1)		
Ca1A–W6	2.58(4)	Ca3A–O6	2.46(2)		

Notes: e.s.d. are reported in parentheses.

hedral double chains, built up through condensation of "Dreiereinfachketten" of wollastonite-type, running along **b** and presenting four twofold connected and two threefold-connected tetrahedra in each unit translation along **b**. The double chains link together two successive calcium polyhedral layers: the doubly connected tetrahedra share an edge with the dome part of the calcium polyhedra and the threefold-connected tetrahedra are linked to the calcium layers through their apical oxygen atoms O6 and O6A. The resulting composite structural scaffolding has composition $(Ca_4Si_6O_{17}\cdot 2H_2O)^{2-}$. (3) The channels running along **b** host one calcium cation and three water molecules for each formula unit, which constitute the "zeolitic" part of the structure, $(Ca\cdot 3H_2O)^{2+}$, leading to the overall crystal chemical formula $Ca_5Si_6O_{17}\cdot 5H_2O$. The calcium cation Ca2 forms strong bonds with three water molecules of the channel, W5, W7, and W8, and two oxygen atoms of the framework, O6 and O4, with three additional weak bonds reported in Table 2.

STRUCTURAL FEATURES OF TOBERMORITE 9 Å

After heating at 225 °C for three hours, a crystal of clinotobermorite topotactically transformed to a new phase, corresponding to the so-called tobermorite 9 Å, namely the phase which may be obtained by heating "normal" tobermorite 11 Å. This phase, too, presents OD character, with the same OD groupoid family as clinotobermorite.

As in clinotobermorite, two MDO polytypes are possible, monoclinic $C2/c$ and triclinic $C\bar{1}$; both polytypes were present in the specimen we obtained in the dehydration process at 225 °C. We collected the reflection data corresponding to the triclinic polytype [a = 11.156(5), b = 7.303(4), c = 9.566(5), α = 101.08(4)°, β = 92.83(5)°, γ = 89.98(4)°], determined and refined the structure to R = 0.144 for 1003 reflections with $F_o > 4\sigma(F_o)$. The structural data are in Tables 3 (atomic coordinates) and 4 (bond distances) and the crystal structure is represented in Figure 4. The calcium layers parallel to (001), which characterize the whole family of tobermorites, are now closer to each other and connected through single chains of wollastonite-type, derived from decondensation of the double chains which are present in clinotobermorite. Four of the five water molecules are lost, the fifth is present as hydroxyl groups SiOH in OH6 position; the different chemical character of O6 and OH6 (oxygen and hydroxyl anions, respectively) is clearly shown by their bond valence sums. The narrow channels of the structure now host only Ca2 calcium cations in positions slightly displaced from the inversion centers at 1/2, 1/2, 1/2, with occupancy 0.5. The resulting crystal chemical formula is $Ca_5Si_6O_{16}(OH)_2$.

STRUCTURAL FEATURES OF TOBERMORITE 11 Å

The general outlines of this structure were sketched more than forty years ago by Megaw and Kelsey (1956), who stud-

TABLE 3. Atomic coordinates and thermal parameters of tobermorite 9 Å, triclinic polytype, space group $C\bar{1}$

Atom	x	y	z	U_{iso} or U_{eq}*
Si1	0.3859(5)	0.2158(8)	0.2234(7)	0.013(1)
Si2	0.3181(6)	–0.0193(9)	0.4343(8)	0.025(2)
Si3	0.3883(5)	0.6416(8)	0.2173(8)	0.015(2)
O1	0.390(2)	0.150(2)	0.377(2)	0.030(4)
O11	0.390(2)	–0.209(2)	0.371(2)	0.024(4)
O2	0.499(2)	0.663(2)	0.121(2)	0.024(4)
O21	0.502(1)	0.152(2)	0.136(2)	0.018(4)
O3	0.268(1)	0.649(2)	0.118(2)	0.013(3)
O31	0.267(2)	0.163(2)	0.133(2)	0.018(4)
O4	0.403(2)	0.441(2)	0.277(2)	0.022(4)
O6	0.179(2)	–0.040(3)	0.384(2)	0.041(5)
OH6	0.152(2)	0.488(3)	0.390(3)	0.050(6)
Ca1	0.3713(4)	0.0981(6)	–0.1040(6)	0.017(1)
Ca2	0.499(1)	0.460(1)	0.502(2)	0.035(3)
Ca3	0.3647(4)	0.5966(6)	–0.1175(6)	0.017(1)

* (Isotropic U for oxygen atoms and Ca2; equivalent U for silicon atoms, Ca1 and Ca3).

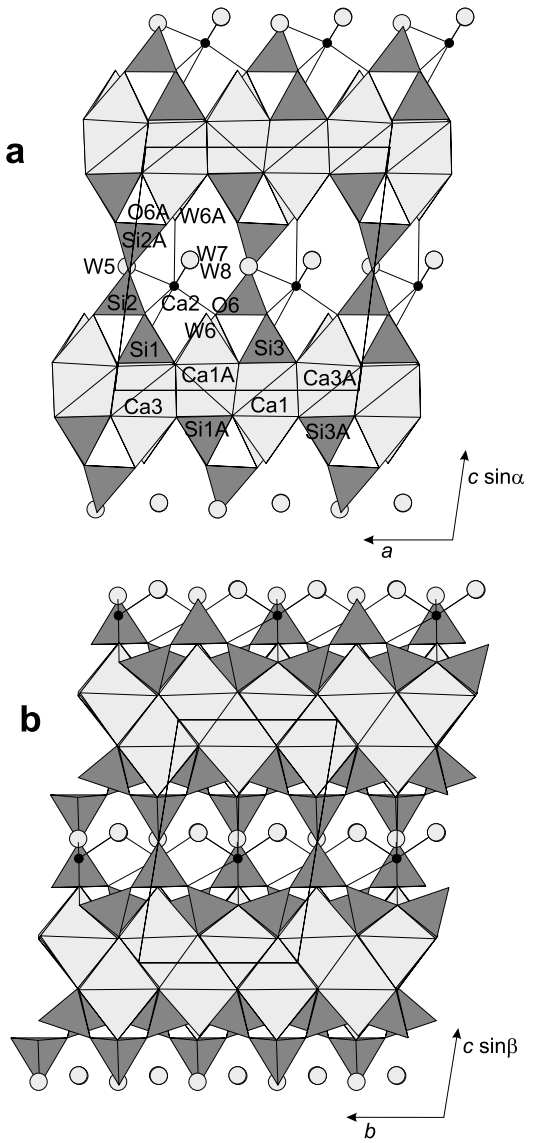

FIGURE 3. Crystal structure of the triclinic polytype MDO_2 of clinotobermorite, as seen along [010] (**a**) and down [100] (**b**). The "framework" is built up by chains of silicon tetrahedra (dark gray) and layers of sevenfold-coordinated calcium polyhedra (light gray). The calcium cation Ca2 is tightly bonded to two oxygen atoms of the framework and to the "zeolitic" water molecules W5, W7 and W8.

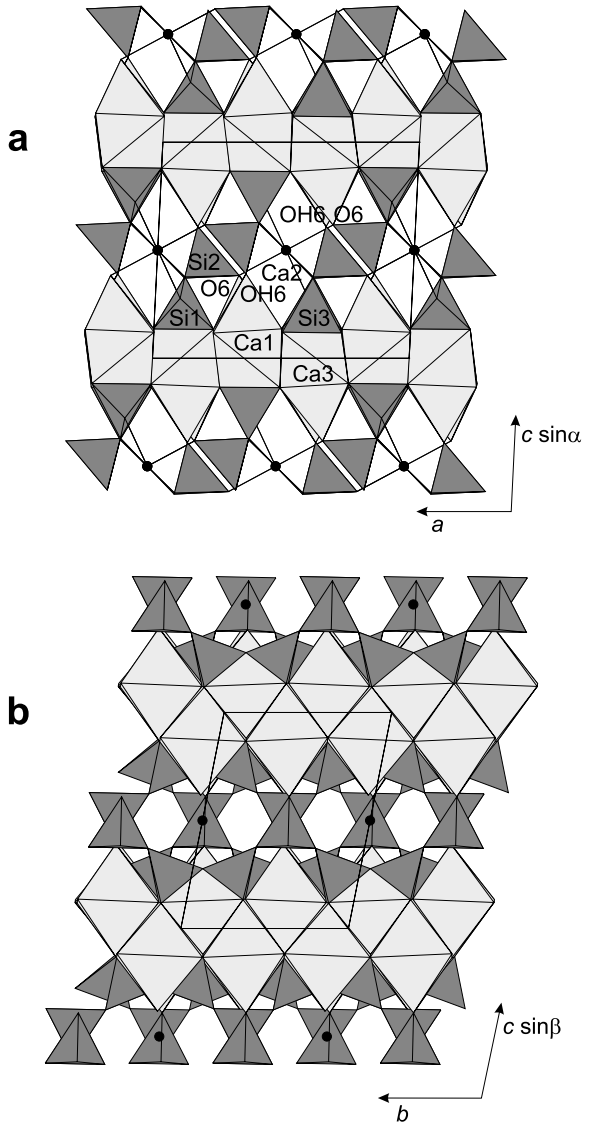

FIGURE 4. Crystal structure of the triclinic polytype MDO_2 of tobermorite 9 Å, as seen down [010] (**a**) and along [100] (**b**). The calcium cation Ca2 is tightly bonded to oxygen atoms of the framework. Symbols are as in Figure 3.

TABLE 4. Selected bond distances (in angstroms) in triclinic tobermorite 9Å

Si1–O1	1.63(2)	Si2–O1	1.67(2)	Si3–O11	1.65(2)
Si1–O21	1.60(2)	Si2–O11	1.63(2)	Si3–O2	1.61(2)
Si1–O31	1.56(2)	Si2–O6	1.61(2)	Si3–O3	1.62(2)
Si1–O4	1.63(2)	Si2–OH6	1.68(2)	Si3–O4	1.68(2)
Ca1–O2	2.30(2)	Ca3–O2	2.43(2)	Ca2–O1	2.62(2)
Ca1–O21	2.29(2)	Ca3–O2	2.65(2)	Ca2–O11	2.67(2)
Ca1–O21	2.63(2)	Ca3–O21	2.41(2)	Ca2–O4	2.32(2)
Ca1–O3	2.36(2)	Ca3–O3	2.38(2)	Ca2–O4	2.35(2)
Ca1–O31	2.38(2)	Ca3–O3	2.52(2)	Ca2–O6	2.34(3)
Ca1–O31	2.57(2)	Ca3–O31	2.38(2)	Ca2–O6	2.36(3)
Ca1–OH6	2.70(2)	Ca3–O6	2.54(2)		

Notes: esd. are reported in parentheses.

ied the subcell structure of a specimen of tobermorite from Ballycraigy. Hamid (1981) refined it in the space group *Imm*2 (a_S = 5.586, b_S = 3.696, c_S = 22.779 Å), with data collected using a specimen from Zeilberg. Both studies pointed to the presence of tetrahedral single chains of wollastonite-type.

The close metrical relationships between clinotobermorite and tobermorite 11 Å and the results obtained in our study of clinotobermorite regarding the average structure and its OD interpretation suggested a reliable structural hypothesis for tobermorite 11 Å. In particular we assumed that in tobermorite 11 Å the double tetrahedral chains are obtained from the single chains through the action of a mirror plane normal to **c**, instead

of through the action of a twofold axis parallel to **b**; therefore we pass from the symmetry *C*12/*m*1 of the single layer of clinotobermorite to a symmetry *C*2*mm* of the single layer in tobermorite 11 Å. On the basis of the data obtained in the structural study of clinotobermorite, the periodicities of the single layer are: $a = 11.2$, $b = 7.3$, width $c_0 = 11.2$ Å.

For a layer with symmetry *C*2*mm* and **c** as the direction of missing periodicity, OD theory suggests two possible OD groupid family groups. One of them

$$C \quad 2 \quad m \quad (m) \qquad (6)$$
$$\{\ 2_{1/2}\ n_{2,1/2}\ (n_{1/2,1/2})\ \}$$

appeared as the correct one as its λ and σ operations closely correspond to the operations of space group *I*2*mm* of the subcell structure (it may be observed that the structure described by Hamid (1981) in space group *Imm*2 may be described also in the space group *I*2*mm*).

The correct set of σ-operations indicates that pairs of successive layers are related by stacking vectors: $\mathbf{t}_1 = \mathbf{c}_0 + (\mathbf{a} + \mathbf{b})/4$ or $\mathbf{t}_2 = \mathbf{c}_0 + (\mathbf{a} - \mathbf{b})/4$. Among the infinite possible disordered or ordered structures (polytypes) corresponding to the infinite disordered or ordered sequences of the two stacking vectors, OD theory singles out two MDO structures, MDO_1 and MDO_2, corresponding to the stacking sequences $\mathbf{t}_1\mathbf{t}_2\mathbf{t}_1\mathbf{t}_2$..... and $\mathbf{t}_1\mathbf{t}_1\mathbf{t}_1\mathbf{t}_1$.... (the stacking sequence $\mathbf{t}_2\mathbf{t}_2\mathbf{t}_2\mathbf{t}_2$.....corresponds to the twin structure MDO_2'). Their unit cell dimensions and space group symmetries, which may be obtained following the same procedures as applied in the case of clinotobermorite, are $a = 11.2$, $b = 7.3$, $c = 44.8$ Å, space group *F*2*dd*, and $a = 6.7$, $b = 7.3$, $c = 22.4$ Å, $\gamma = 123°$, space group *B*11*m* (the unit-cell parameters of the monoclinic cell are given in a non-standard orientation), respectively.

Extraordinarily well developed crystals of tobermorite 11 Å from the Wessels mine (the same locality where the crystals of clinotobermorite used in our structural study were found) provided a reliable test of our model. Their X-ray diffraction pattern closely corresponds to that found by McConnell (1954) in his study of tobermorite 11 Å from Ballycraigy: reflections with odd *k* values are weak and diffuse, the direction of the spreading being along **c***. Reflections with even *k* values are always sharp; they correspond to the family reflections and point to a subcell with $a = 5.633$, $b = 3.692$, $c = 22.487$ Å. The subcell structure was determined and refined in the space group *I*2*mm*, in agreement with the indications of our model.

The distribution of the reflections with odd *k* values in the reciprocal space showed that both MDO polytypes, with both twin orientations of the polytype MDO_2, were present. X-ray diffraction data were collected from the largest twin individual of the monoclinic polytype ($a = 6.735$, $b = 7.385$, $c = 22.487$ Å, $\gamma = 123.25°$; space group *B*11*m*) and the structure has been refined to $R = 0.051$ [1648 reflections with $F_o > 4\sigma(F_o)$]. The results are given in Tables 5 (atomic coordinates) and 6 (bond distances) and the structural arrangement is represented in Figure 5.

The infinite layers of sevenfold-coordinated calcium polyhedra parallel to (001) are quite similar to those already found in clinotobermorite and tobermorite 9 Å; the only difference lies in the apical sites of the pyramidal parts of the calcium polyhedra, where hydroxyl anions OH6 and water molecules W6 regularly alternate along **b**, to compare with the alternation of oxygen atoms and water molecules in clinotobermorite and oxygen atoms and hydroxyl anions in tobermorite 9 Å.

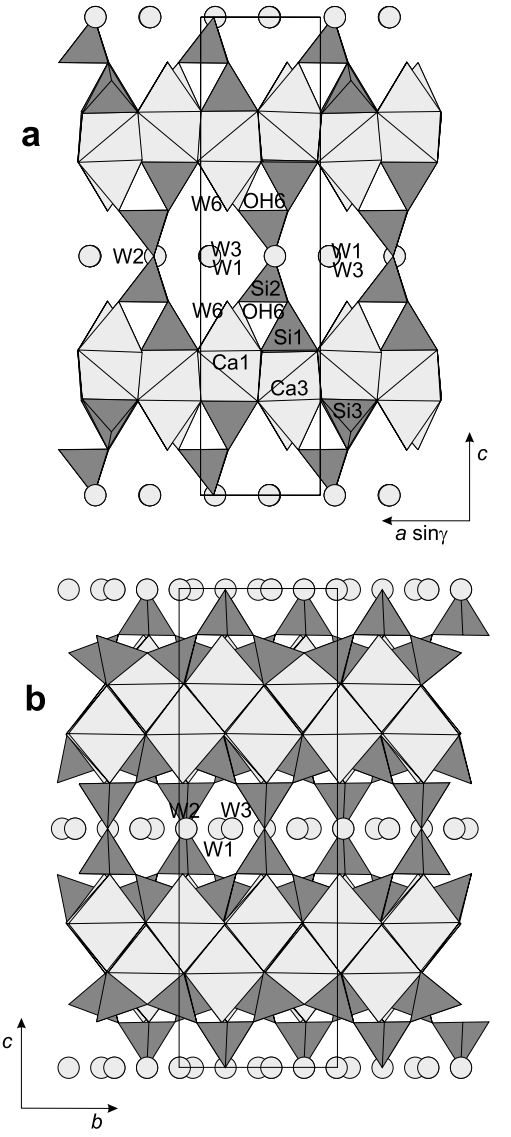

FIGURE 5. Crystal structure of the monoclinic polytype MDO_2 of tobermorite 11 Å from the Wessels mine, as seen along [010] (**a**) and down [210] (**b**). Symbols are as in Figure 3.

As in clinotobermorite, tetrahedral double chains, built up through condensation of "Dreiereinfachketten" of wollastonite-type, run along **b** and link together two successive calcium polyhedral layers. However they present a peculiar C-shape, as seen along [010], displaying 2*mm* symmetry, to compare with the 2/*m* symmetry of the corresponding double chains in clinotobermorite. The resulting composite framework has composition $Ca_4Si_6O_{15}(OH)_2 \cdot 2H_2O$.

The described scaffolding presents wide channels running along **b**: they may host calcium cations and water molecules. In the specimen of tobermorite 11 Å from the Wessels mine,

Table 5. Atomic coordinates and thermal parameters for tobermorite 11 Å, monoclinic polytype, space group *B*11*m*.

Atom	*x*	*y*	*z*	U_{eq} or U_{iso}*
Si1	0.7581(4)	0.3862(3)	0.15738(7)	0.0054(3)
Si2	0.9087(4)	0.7531(3)	0.07116(7)	0.0086(3)
Si3	0.7592(4)	0.9697(3)	0.15773(8)	0.0056(3)
O1	0.771(1)	0.5059(8)	0.0942(2)	0.014(1)
O2	0.759(1)	0.178(1)	0.1327(2)	0.0127(8)
O3	0.985(1)	0.5369(9)	0.1982(2)	0.0090(9)
O4	0.519(1)	0.3063(8)	0.1942(2)	0.012(1)
O5	0.894(2)	0.746(1)	0.0	0.017(1)
OH6	0.188(1)	0.893(1)	0.0940(2)	0.018(1)
W6	0.270(2)	0.434(2)	0.0939(3)	0.045(2)
O7	0.770(1)	0.860(1)	0.0951(2)	0.015(1)
O8	0.523(1)	0.8110(8)	0.1951(2)	0.011(1)
O9	0.987(1)	0.0459(9)	0.1985(2)	0.010(1)
Ca1	0.2651(2)	0.4328(2)	0.20557(6)	0.0085(3)
Ca3	0.7499(2)	0.9228(2)	0.29348(5)	0.0074(3)
W1	0.427(5)	0.219(5)	0.0	0.14(1)
W2	0.879(3)	0.237(3)	0.0	0.061(4)
W3	0.422(5)	0.800(5)	0.0	0.13(1)

* (isotropic *U* for W1, W2, and W3, equivalent *U* for all the others).

TABLE 6. Bond distances in tobermorite 11 Å, monoclinic polytype

Si1–O1	1.649(5)	Si2–O1	1.614(5)	Si3–O2	1.640(6)
Si1–O2	1.637(6)	Si2–O5	1.603(2)	Si3–O7	1.646(5)
Si1–O3	1.599(6)	Si2–OH6	1.654(6)	Si3–O8	1.602(6)
Si1–O4	1.609(7)	Si2–O7	1.612(6)	Si3–O9	1.601(6)
Ca1–O3	2.399(6)	Ca3–O3	2.400(6)		
Ca1–O3	2.495(6)	Ca3–O4	2.398(5)		
Ca1–O4	2.368(6)	Ca3–OH6	2.555(6)		
Ca1–O4	2.647(6)	Ca3–O8	2.407(6)		
Ca1–W6	2.511(7)	Ca3–O8	2.556(6)		
Ca1–O8	2.356(5)	Ca3–O9	2.400(6)		
Ca1–O9	2.414(6)	Ca3–O9	2.520(6)		

Notes: esd are reported in parentheses.

three water molecules and no calcium cations were found there in the present structural study. The overall crystal chemical formula is therefore: $Ca_4Si_6O_{15}(OH)_2 \cdot 5H_2O$.

The list of F_o and F_c for the three structures of Figures 3, 4, and 5, can be found in Table 7.[2]

CONSIDERATIONS

Zadov et al. (1995) indicated that the compositions of natural tobermorites present CaO/SiO_2 molar ratios between 5/6 and 4/6. From the above structural results for tobermorite 11 Å and clinotobermorite, we propose the following extreme formulations for the composition of tobermorite 11 Å: $Ca_4Si_6O_{15}(OH)_2 \cdot 5H_2O$ and $Ca_5Si_6O_{17} \cdot 5H_2O$, with the general formula $Ca_{4+x}Si_6O_{15+2x}(OH)_{2-2x} \cdot 5H_2O$. The composition of the specimen from the Wessels mine approximates the first formulation. It may not be completely excluded that a small amount of calcium cations are located in the cavities, the small excess positive charge being compensated by corresponding Al to Si or/and O^{2-} to OH^- partial substitutions.

This refinement presents the first direct evidence of the presence of condensed wollastonite chains in tobermorite 11 Å, together with information on the distribution of the water molecules in the channels and on the rules governing the layer stacking. The presence of Si-O-Si bridges connecting wollastonite chains facing each other was firstly suggested by Mitsuda and Taylor (1979) to explain the "anomalous" behavior in some specimens of tobermorite 11 Å and was subsequently confirmed through chemical methods (Winkler and Wieker 1979) and ^{29}Si MASNMR studies (Wieker et al. 1982; Komarneni et al. 1985; Mitsuda et al. 1989). The preceding X-ray diffraction studies by Megaw and Kelsey (1956) and Hamid (1981), carried on specimens of tobermorite from Ballycraigy and Zeilberg, respectively, pointed to single wollastonite chains.

The particular specimen we have studied does not shrink on heating, thus appearing an "anomalous" type. However the diffraction patterns it displays, and in particular the space group of the subcell reflections ("family reflections"), is the same as found by McConnell (1954) for "normal" tobermorite from Ballycraigy and by Hamid (1981) for tobermorite from Zeilberg. Consequently we retain that also "normal" tobermorite from Ballycraigy (and tobermorite from Zeilberg as well) present the same OD features and the same structure of the single layer as displayed by tobermorite from the Wessels mine. The different behavior on dehydration cannot be explained assuming condensed and single wollastonite chains in "anomalous" and "normal" tobermorite, respectively. In fact, this kind of explanation is untenable since we have demonstrated that clinotobermorite, which presents condensed chains, easily and quickly shrinks to tobermorite 9 Å on dehydration.

The explanation we present for the different behavior of distinct specimens of tobermorite 11 Å is based on the comparison of the crystal structures of clinotobermorite and tobermorite 11 Å from the Wessels mine. In clinotobermorite, $Ca_5Si_6O_{17} \cdot 5H_2O$, the "zeolitic" calcium cation is tightly bonded to three water molecules which are lost in the dehydration process. This has severe consequences on the stability of the crystal structure and causes a general rearrangement: chain-decondensation and generation of tobermorite 9 Å, in which the calcium cation forms six strong bonds with the oxygen atoms. On the other hand there are no (or very few) "zeolitic" calcium cations in the structure of tobermorite 11 Å from the Wessels mine. Therefore the loss of water in the dehydration process has no severe consequence on the whole structure and no rearrangement is required.

In the case of a specimen of tobermorite 11 Å with composition $Ca_5Si_6O_{17} \cdot 5H_2O$ to $Ca_5Si_5AlO_{16}(OH) \cdot 5H_2O$ (the Al to Si substitution is frequent in natural tobermorites, with a maximum Al/(Si + Al) ratio of 1/6, compensated by corresponding OH^- to O^{2-} substitution) the situation should probably be the same as in the case of clinotobermorite and correspondingly it would have the behavior of "normal" tobermorite.

ACKNOWLEDGMENTS

This work was supported by MURST (Ministero dell'Università e della Ricerca Scientifica) through a grant to the national project "Relations between structure and properties in minerals: analysis and applications." The tobermorite crystals from the Wessels mine were kindly provided by Jens Gutzmer (Rand Afrikaans University, Johannesburg, RSA) who is highly acknowledged.

[2]For a copy of Table 7, Document item AM-99-027, contact the Business Office of the Mineralogical Society of America (see inside front cover of recent issue) for price information. Deposit items may also be available on the American Mineralogist web site at http://www.minsocam.org.

REFERENCES CITED

Dornberger-Schiff, K. (1956) On the order-disorder (OD-structures). Acta Crystallographica 9, 593.

———(1964). Grundzüge einer Theorie von OD-Strukturen aus Schichten. Abhandlungen der Deutschen Akademie der Wissenschaften zu Berlin. Klasse für Chemie, Geologie und Biologie, 3, 1–107.

———(1966) Lehrgang über OD-Strukturen, Akademie-Verlag, Berlin.

Dornberger-Schiff, K. and Fichtner, K. (1972) On the symmetry of OD-structures consisting of equivalent layers. Kristall und Technik, 7, 1035–1056.

Ďurovič, S. (1997) Fundamentals of the OD theory. In S. Merlino, Ed., Modular aspects of minerals, EMU Notes in Mineralogy, 1, 3–28. Eötvös University Press, Budapest.

Hamid, S.A. (1981) The crystal structure of the 11 Å natural tobermorite $Ca_{2.25}[Si_3O_{7.5}(OH)_{1.5}]\cdot 1H_2O$. Zeitschrift für Kristallographie, 154, 189–198.

Henmi, C. and Kusachi, I. (1992) Clinotobermorite, $Ca_5Si_6(O,OH)_{18}\cdot 5H_2O$, a new mineral from Fuka, Okayama Prefecture, Japan. Mineralogical Magazine, 56, 353–358.

Hoffmann, C. and Armbruster, T. (1997) Clinotobermorite, $Ca_5[Si_3O_8(OH)_2\cdot 4H_2O - Ca_5[Si_6O_{17}]\cdot 5H_2O$, a natural C-S-H(I) cement mineral: determination of the substructure. Zeitschrift für Kristallographie 212, 864–873.

Komarneni, S. and Roy, D.M.(1983) Tobermorites: a new family of cation exchangers. Science, 221, 647–648.

Komarneni, S., Roy, R., Roy, D.M., Fyfe, C.A., Kennedy, G.J., Bothner-By, A.A., Dadok, J., and Chesnik, A.S. (1985) ^{27}Al and ^{29}Si magic angle spinning nuclear magnetic resonance spectroscopy of Al-substituted tobermorites. Journal of Materials Science, 20, 4209–4214.

McConnell, J.D.C. (1954) The hydrated calcium silicates riversideite, tobermorite, and plombierite. Mineralogical Magazine, 30, 293–305.

Megaw, H.D. and Kelsey, C.H. (1956) Crystal structure of tobermorite. Nature, 177, 390–391.

Merlino, S. (1997) OD approach in minerals. In S. Merlino, Ed., Modular aspects of minerals, EMU Notes in Mineralogy, 1, 3–28. Eötvös University Press, Budapest.

Mitsuda, T. and Taylor, H.F.W. (1979) Normal and anomalous tobermorites. Mineralogical Magazine, 42, 229–235.

Mitsuda, T., Toraya, H., Okada, Y., and Shimoda, M. (1989) Synthesis of tobermorite: NMR spectroscopy and analytical electron microscopy. Ceramic Transactions, 3, 206–213.

Taylor, H.F.W. (1964) The calcium silicate hydrates. In H.F.W. Taylor, Ed., The Chemistry of Cements, p. 167–232. Academic Press, London.

———(1992) Tobermorite, jennite, and cement gel. Zeitschrift für Kristallographie, 202, 41–50.

———(1997) Cement Chemistry, 2nd edition. Thomas Telford Publishing, London.

Wieker, W., Grimmer, A.R., Winkler, A., Magi, M., Tarmak, M., and Lippmaa, E. (1982) Solid-state High-resolution ^{29}Si NMR Spectroscopy of synthetic 14Å, 11Å, and 9Å tobermorites. Cement and Concrete Research, 12, 333–339.

Winkler, A. and Wieker, W. (1979) Uber Synthese, Aufbau und thermisches Verhalten von 11A-Tobermorit. Zeitschrift der anorganische und allgemeine Chemie, 451, 45–56.

Zadov, A.E., Chukanov, N.V., Organova, N.I., Belakovsky, D.I., Fedorov, A.V., Kartashov, P.M., Kuzmina, O.V., Litzarev, M.A., Mokhov, A.V., Loskutov, A.B., and Finko, V.I. (1995) The new findings and study of the tobermorite group minerals. Proceedings of the Russian Mineralogical Society, 124, 36–54 (in Russian).

MANUSCRIPT RECEIVED DECEMBER 28, 1998
MANUSCRIPT ACCEPTED JUNE 24, 1999
PAPER HANDLED BY JAMES W. DOWNS